Available online at www.sciencedirect.com
ScienceDirect
Bioorganic & Medicinal Chemistry 15 (2007) 7021–7034
Bioorganic & Medicinal Chemistry

Antiproliferative activity of chalcones with basic functionalities

Xiaoling Liu and Mei-Lin Go*

Department of Pharmacy, National University of Singapore, 18 Science Drive 4, Singapore 117543, Singapore

Received 30 May 2007; revised 18 July 2007; accepted 20 July 2007
Available online 21 August 2007

Abstract—A library of chalcones with different basic groups were synthesized and evaluated for antiproliferative activities against the human breast cancer (MCF 7) and colon cancer (HCT 116) cell lines. Structure–activity relationships were analyzed by projection methods (PCA/PLS) and multiple linear regression. Polar volume, hydrogen bonding features, HOMO energies, and charge on the β carbon were found to be important factors. A basic group on either ring A or B of the chalcone led to a favourable increase in polar volume, but when present on ring B, it increased HOMO energies and decreased the positive charge on the β carbon, both of which led to lower activity. Several examples showed that final activity of the chalcone was influenced by compensatory interactions among these parameters. In general, a single basic group on ring A was associated with good activity. A notable exception was compound **1-123** which had basic groups on both rings A and B but still maintained a good activity profile with $IC_{50} < 10$ μM and selectivity ratios >2.5. There was some evidence to show that structural differences in chalcones influenced not only activity but mechanism of action. Compounds **6-130** and **7-140** which had basic groups on ring A interfered with cell cycle progression, but the dibasic chalcone **1-123** had no effect.

1. Introduction

There are several reports on the antiproliferative properties of chalcones substituted with basic groups. Xia and coworkers[1] were among the first to demonstrate the improved antiproliferative activity of chalcones with amino groups. Pati et al.[2] showed that methoxylated chalcones with a 3′-amino group had submicromolar IC_{50} values against murine melanoma B16 cells. Dimmock and coworkers[3] proposed that the presence of amino function would increase the reactivity of chalcones as Michael acceptors and thus their antiproliferative activity. They postulated that the amino function would be protonated at the low pH environment normally encountered in tumors. The electron withdrawing effect of the protonated ammonium function would enhance the electrophilicity of the β carbon in the enone linkage, hence increasing its reactivity as a Michael acceptor. In our earlier investigation,[4] we focused on piperidinyl chalcones as antiproliferative agents, partly because heterocycles like piperidine were less likely to form reactive metabolites compared to the primary amino function favored by other investigators.[1–3] Many of the piperidinyl chalcones had promising antiproliferative activities ($IC_{50} \leqslant 5$ μM) and disrupted the cell cycle at G1 and G2/M phases at these concentrations. In contrast, chalcones without the basic substituent had no effect on the cell cycle when tested at their IC_{50}. In view of this finding, we proceeded to synthesize a larger library of chalcones bearing different basic substituents. The compounds were evaluated for antiproliferative activities on two human cancer cell lines. Our objectives were to assess how the presence of the basic moiety influenced the physicochemical profile of the chalcone, and if this would in turn affect antiproliferative activity. To address these issues, the compounds were characterized by a wide range of physicochemical descriptors and their structure–activity relationships were analyzed by projection methods and multiple linear regression.

2. Design and synthesis

The chalcones were classified into groups according to their substitution patterns on ring A (Table 1). Group 1 chalcones had ring A substituted with methoxy groups at positions 2 and 4, and 1-methylpiperidin-4-yl at position 5. Groups 6, 7 and 8 were variants of Group 1 in which 1-methylpiperidin-4-yl had been replaced by groups of comparable basicities, namely 1-ethylpiperidine (Group 6), 1-methylpiperazine (Group 7) and 4-(1-pipe-

Keywords: Chalcones with basic functionalities; Antiproliferative activity; Structure–activity relationship.
* Corresponding author. Tel.: +65 65162654; fax: +65 67791554; e-mail: phagoml@nus.edu.sg

0968-0896/$ - see front matter © 2007 Elsevier Ltd. All rights reserved.
doi:10.1016/j.bmc.2007.07.042

Table 1. IC_{50} (μM) values and selectivity ratios (SR) of synthesized chalcones

Code	Ring A[a]	R′ on ring B[a]	$IC_{50\,MCF7}$[b]	SR_{MCF}[c]	$IC_{50\,HCT116}$[b]	SR_{HCT}[c]	$IC_{50\,CCL186}$[b]
1-5		2′-Cl	2.8 ± 0.4	2.7	3.4 ± 0.0	2.2	7.6 ± 0.9
1-6		H	3.4 ± 0.7	2.3	3.9 ± 0.2	2.0	7.8 ± 1.7
1-7	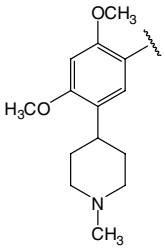	4′-Cl	2.5 ± 0.6	1.4	2.9 ± 0.5	1.2	3.6 ± 0.4
1-120		Pyridin-4-yl[d]	7.2 ± 0.3	1.9	9.9 ± 2.6	1.4	13.9 ± 0.5
1-121		Pyridin-3-yl[d]	4.3 ± 1.1	3.0	7.4 ± 2.1	1.7	12.9 ± 1.6
1-122		Pyridin-2-yl[d]	3.9 ± 0.6	2.7	12.4 ± 1.6	0.9	10.6 ± 2.5
1-123		4′-MPZ[e]	8.5 ± 1.9	2.7	7.8 ± 1.8	2.9	22.7 ± 3.7
1-60		2′-CH_3	6.6 ± 0.7	1.6	10.2 ± 1.3	1.0	10.3 ± 1.0
1-61		4′-CH_3	5.4 ± 0.5	1.6	10.4 ± 1.8	0.9	8.8 ± 1.5
1-62		2′-CH_3O	7.0 ± 0.8	1.8	9.4 ± 1.1	1.3	12.5 ± 1.4
1-63		4′-CH_3O	7.0 ± 1.6	2.4	17.7 ± 6.7	0.9	16.7 ± 5.0
1-64	GROUP 1	2′-F	3.8 ± 0.4	3.5	10.3 ± 2.9	1.3	13.2 ± 3.0
1-65		4′-F	3.9 ± 0.5	2.3	8.3 ± 3.9	1.1	9 ± 2.7
1-66		4′-CF_3	2.8 ± 0.3	2.1	8.7 ± 3.1	0.7	6 ± 0.5
2-17		2′-Cl	3.1 ± 0.3	1.0	3.1 ± 0.9	1.0	3.1 ± 1.5
2-2		4′-Cl	6.7 ± 0.3	0.9	2.6 ± 1.3	2.4	6.1 ± 2.7
2-3		H	5.7 ± 1.1	1.3	4.2 ± 1.6	1.7	7.3 ± 0.0
2-4	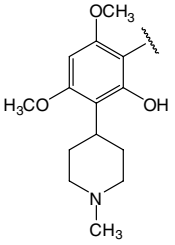	2′-F	3.4 ± 0.0	1.4	3.0 ± 0.5	1.5	4.6 ± 1.0
2-50		4′-F	6.4 ± 0.8	1.4	8.6 ± 2.6	1.0	8.9 ± 1.6
2-51		2′-CH_3	22.3 ± 1.4[g]	0.5	18.3 ± 7.9	0.6	10.4 ± 1.3
2-52		4′-CH_3	6.6 ± 0.2	0.4	7.0 ± 2.6	0.4	2.9 ± 0.6
2-53		2′-CH_3O	10.1 ± 0.7	0.7	10.2 ± 3.0	0.7	6.6 ± 0.6
2-54		4′-CH_3O	25.5 ± 2.7[g]	0.4	16 ± 2.6[g]	0.6	9.7 ± 3.8
2-55		3′-CH_3O 1	31.2 ± 5.1[g]	1.6	50[f,g]	1.0	50[f]
2-56		2′,4′-$(CH_3O)_2$	12.1 ± 1.3[g]	0.4	6.6 ± 1.7	0.7	4.4 ± 0.9
2-57	GROUP 2	3′-Cl	2.7 ± 0.6	0.8	7.4 ± 0.5	0.3	2.2 ± 0.6
2-58		4′-CN	13.8 ± 0.9[g]	2.7	25.8 ± 0.6[g]	1.5	37.7 ± 3.7
2-59		4′-CF_3	14.3 ± 0.3[g]	1.3	17.8 ± 2.1[g]	1.0	18 ± 3.4
2-124		4′-MPZ[e]	14.4 ± 1.4[g]	0.7	13.9 ± 1.6[g]	0.7	9.4 ± 1.9
2-59a		4′-$(CH_3)_2N$	13.9 ± 0.8[g]	0.6	26.6 ± 1.2[g]	0.3	7.9 ± 0.8
3-100		2′ ,4′-$(CH_3O)_2$	16.3 ± 3.0[g]	1.4	13.4 ± 3.0	1.7	22.2 ± 5.2
3-101	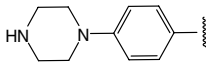	2′-Cl	21.4 ± 0.5[g]	1.2	10.5 ± 7.8	2.5	26.6 ± 2.8
3-102		4′-Cl	8.5 ± 1.4	1.3	4.9 ± 1.9	2.3	11.3 ± 3.4
3-103	GROUP 3	H	50[g]	1.0	50[f,g]	1.0	50[f]
4-104		2′-Cl	47.4 ± 4.9[g]	1.1	23.9 ± 6.8[g]	2.1	50[f]
4-105	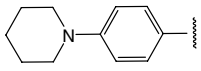	4′-Cl	25.1 ± 0.7[g]	2.0	50[f,g]	1.0	50[f]
4-106		H	50[f,g]	1.0	50[f,g]	1.0	50[f]
4-107	GROUP 4	2′,4′-$(CH_3O)_2$	50[f,g]	1.0	50[f,g]	1.0	50[f]
5-14		4′-Cl	6.5 ± 1.3	1.7	6.2 ± 1.2	1.8	11.3 ± 0.7
5-15	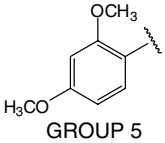	2′-Cl	ND	—	5.2 ± 0.6	2.5	12.8 ± 0.6
5-16		H	ND	—	4.4 ± 0.7	3.1	13.7 ± 0.8
5-110		Pyridin-4-yl[d]	7.9 ± 0.6	2.6	12 ± 9.1	1.7	20.5 ± 5.1
5-111		Pyridin-3-yl[d]	13.6 ± 2.8	2.7	22.1 ± 12.1	1.7	36.9 ± 8.9
5-112		Pyridin-2-yl[d]	6.4 ± 2.0	2.2	18.9 ± 6.6	0.8	14.1 ± 2.2
5-113	GROUP 5	4′-MPZ[e]	13.7 ± 1.8[g]	3.3	17 ± 4.6	2.6	44.8 ± 5.1
6-130		2′-Cl	2.6 ± 0.5	3.9	6.7 ± 2.1	1.5	10 ± 0.9
6-131	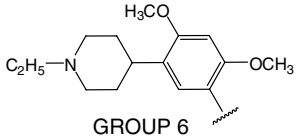	H	4.8 ± 1.4	3.7	7.7 ± 1.6	2.3	17.5 ± 1.8
6-132		4′-Cl	3.4 ± 0.3	2.3	6.8 ± 1.6	1.2	7.8 ± 2.3
6-133		Pyridin-4-yl[d]	2.9 ± 1.3	2.3	7.5 ± 3.0	0.9	6.6 ± 0.3
6-134	GROUP 6	4′-MPZ[e]	8.8 ± 3.5	2.3	10 ± 2.7	2.0	20.4 ± 1.2
7-140		2′-Cl	6.2 ± 0.6	2.5	14.1 ± 0.7[g]	1.1	15.4 ± 0.7
7-141	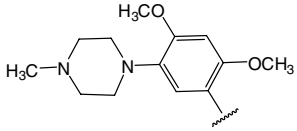	2′-F	7.2 ± 0.4	2.3	16.7 ± 1.8[g]	1.0	16.6 ± 1.7
7-142		H	6.0 ± 1.4	2.6	19.4 ± 2.0[g]	0.8	15.7 ± 1.7
7-143		4′-MPZ[e]	13.8 ± 2.4[g]	3.4	40.4 ± 6.1[g]	1.2	47 ± 2.6
7-144	GROUP 7	Pyridin-4-yl[d]	12.4 ± 2.1	2.2	29.8 ± 0.8[g]	0.9	27.1 ± 0.9

Table 1 (*continued*)

Code	Ring A[a]	R′ on ring B[a]	$IC_{50\,MCF7}$[b]	SR_{MCF}[c]	$IC_{50\,HCT116}$[b]	SR_{HCT}[c]	$IC_{50\,CCL186}$[b]
8-160	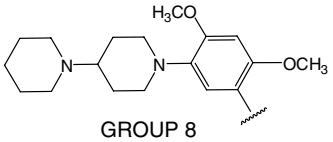 GROUP 8	2′-Cl	3.7 ± 0.3	1.8	19.3 ± 8.6	0.3	6.5 ± 0.7
8-161		2′-F	3.5 ± 0.2	2.0	16.8 ± 4.9	0.4	6.9 ± 0.2
9-150	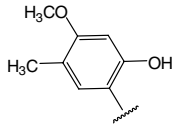 GROUP 9	2′-Cl	22.4± 5.7[g]	0.9	50[f,g]	0.4	19.2 ± 1.0
9-151		2′-CH_3O	11.8 ± 0.1[g]	1.0	50[f,g]	0.2	11.8 ± 3.8
9-152		H	25.5 ± 0.9[g]	0.7	37.3 ± 2.4[g]	0.5	18.6 ± 0.5
10-8	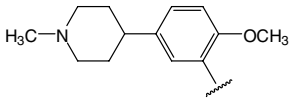 GROUP 10	2′-Cl	2.9 ± 0.2	2.1	2.3 ± 0.7	2.6	6 ± 0.1
10-9		4′-Cl	3.2 ± 0.1	1.6	3.3 ± 0.7	1.6	5.2 ± 0.1
10-10		H	4.2 ± 0.3	2.3	3.6 ± 1.2	2.7	9.8 ± 1.0
11-11	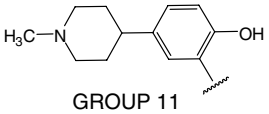 GROUP 11	2′-Cl	ND	—	6.9 ± 0.6	2.2	15.3 ± 0.6
13	2,3,4-Trimethoxy phenyl	2′,4′-$(CH_3O)_2$	ND	—	25.1 ± 2.6[g]	1.2	30.0 ± 2.8

ND, not determined.

[a] Rings A and B refer to the rings in the chalcone template:

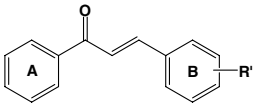

.

[b] IC_{50} values were determined against the human breast cancer cells MCF 7, transformed human colon cancer cells HCT 116, and normal human diploid embryonic lung fibroblasts CCL 186. Values represent the mean of at least two determinations.

[c] Selectivity ratio = $IC_{50\,CCL186}/IC_{50\,MCF7}$ or $IC_{50\,CCL186}/IC_{50\,HCT116}$.

[d] Ring B of chalcone is replaced by pyridine.

[e] 4′-MPZ = 4′-(4-methylpiperazin-1-yl).

[f] Values were not accurately determined and IC_{50} is likely to exceed 50 μM.

[g] Significantly greater than 10 μM, independent samples *t*-test, $p < 0.05$.

ridinyl) piperidine (Group 8). Addition of a phenolic OH group to ring A of Group 1 gave the Group 2 chalcones and removal of 4-methoxy from ring A of Group 1 gave the Group 10 chalcones. Groups 3 and 4 had only basic functionalities on ring A and served to highlight the importance of the omitted methoxy groups on this ring. In contrast, Groups 5 and 9 with no basic substituent on ring A would provide insight on the role of the basic moiety. Demethylation of the methoxy group in Group 10 gave rise to Group 11.

The main substituents on ring B were the halogens (F and Cl) which were associated with good activity in our earlier study.[4] Other substituents were selected from the four quadrants of the Craig Plot,[5] so as to cover a range of π (lipophilicity) and σ (electron donating/withdrawing) values. Most of these substituents were introduced to ring B of Groups 1 and 2. Ring B was also replaced by pyridine, a weakly basic heteroaromatic ring in some compounds.

The chalcones were synthesized by a base-catalyzed Claisen Schmidt reaction between a substituted benzaldehyde and a substituted acetophenone (Fig. 1). Mechanistically, the reaction involves formation of a carbanion from the acetophenone in the presence of the base NaOH, followed by nucleophilic attack by the carbanion on the carbonyl carbon of the benzaldehyde and subsequent loss of water to give the chalcone. The benzaldehydes were purchased from commercial sources, except for 4-(4-methylpiperazin-1-yl) benzaldehyde which was synthesized by a palladium-catalyzed reaction between 2-(4-bromophenyl)-1,3-dioxane and 1-methylpiperazine (Fig. 2).[6] The aldehyde functionality of 4-bromobenzaldehyde was first protected by conversion to an acetal before reaction with 1-methylpiperazine. The product was subsequently deprotected in aqueous acid and condensed with the desired acetophenone to give the chalcone.

The syntheses of the acetophenones 1-(2,4-dimethoxy-5-(1-methylpiperidin-4-yl)phenyl)ethanone (**1-1**), 1-(2-hydroxy-4,6-dimethoxy-3-(1-methylpiperidin-4-yl)phenyl) ethanone (**2-1**), and 1-(2-methoxy-5-(1-methylpiperidin-4-yl)phenyl)ethanone (**10-1**) had been described earlier.[4]

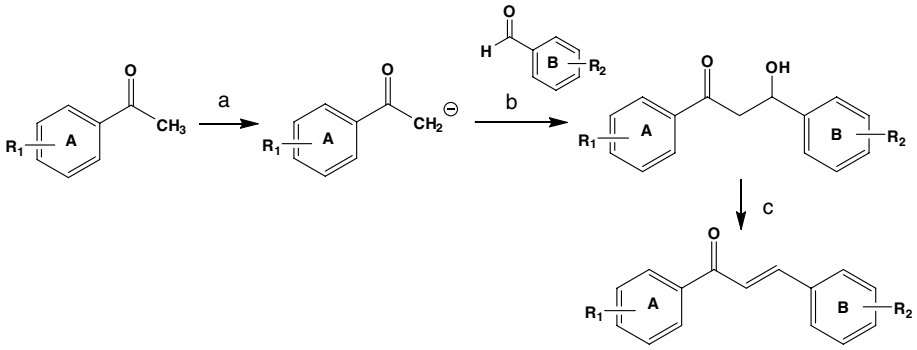

Figure 1. Scheme for synthesis of chalcones, 3% w/v NaOH in methanol, 12 h, rt (28 °C). (a) Formation of carbanion in presence of alkali; (b) reaction with benzaldehyde; (c) loss of water.

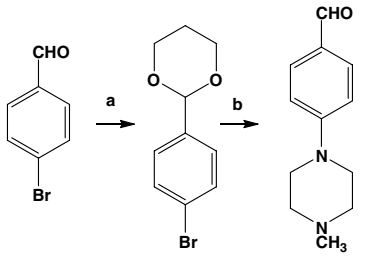

Figure 2. Reagents and conditions: (a) 1,3-propandiol, *p*-TsOH, toluene, reflux, 24 h; (b) (i) $Pd_2(dba)_3$ sodium tertiary butoxide, toluene, reflux 10 h; (ii) aq 1 M HCl.

These acetophenones were used for the syntheses of Groups 1, 2, and 10 chalcones, respectively. 1-(2,4-Dimethoxy-5-(1-ethylpiperidin-4-yl)phenyl)ethanone (**6-1**), the starting acetophenone for Group 6, was synthesized by a similar route (Fig. 3). In the case of Groups 3, 4, and 5, their starting acetophenones were purchased from commercial sources.

1-(2,4-Dimethoxy-5-(4-methylpiperazin-1-yl)phenyl)ethanone (**7-1**) and 1-[5-(1,4′-dipiperidin-1′-yl)-2,4-dimethoxyphenyl]ethanone (**8-1**) were synthesized by Pd/BINAP-catalyzed amination. Briefly, 1-bromo-2,4-dimethoxybenzene was acylated to give the acetophenone which was then reacted with 1-methylpiperazine or 1,4′-bipiperidine in the presence of cesium carbonate as base, $Pd_2(DBA)_3$, and rac-BINAP to give the desired product (Fig. 4).[7] These acetophenones were used for the syntheses of Groups 7 and 8 chalcones.

Compounds **9-1** and **11-1** were not intentionally targeted for synthesis but were obtained during the syntheses of other acetophenones. Compound **9-1** was obtained when the synthesis of 1-[5-(diethylaminomethyl)-2,4-dimethoxy phenyl]ethanone was attempted. As shown in Figure 5, the reaction was to proceed via the reduction of *N*,*N*-diethyl-2,4-dimethoxybenzamide to give *N*-(2,4-dimethoxybenzyl)-*N*-ethylethanamine, followed by acetylation with acetic anhydride and boron triflouride to give the desired product. However, the Friedal Crafts reaction resulted in the demethylation of one of the methoxy groups and loss of the diethylamino function to give 1-(2-hydroxy-4-methoxy-5-methylphenyl)ethanone (**9-1**). It was subsequently used as the starting acetophenone for the Group 9 chalcones.

1-(2-Hydroxy-5-(1-methylpiperidin-4-yl)phenyl)ethanone (**11-1**) was obtained during the Friedal Crafts acetylation of 1-methyl-4-(4′methoxyphenyl)piperidine using $AlCl_3$ as the Lewis acid catalyst (Fig. 6). During this reaction, demethylation of the methoxy group occurred. When the catalyst was changed to boron trifluoride, demethylation was not observed and compound **10-1** was obtained[4] (Fig. 6).

3. Results and discussion

3.1. Structure–activity relationships

Table 1 lists the IC_{50} values of the chalcones against human cancer cell lines (breast cancer cells MCF 7 and

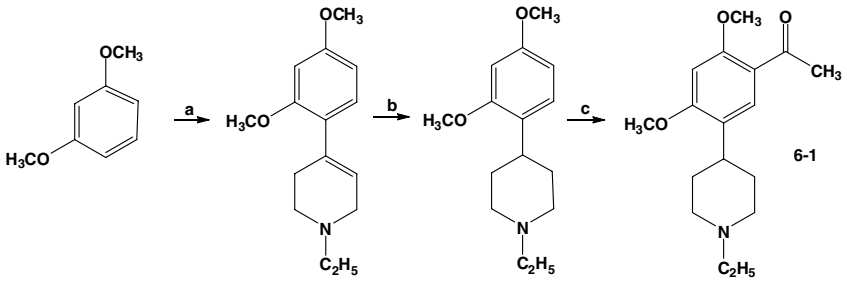

Figure 3. Reagents and conditions: (a) 1-ethylpiperidin-4-one, HCl gas, acetic acid, 25 °C, 24 h; (b) 10% Pd/C, H_2, acetic acid–water, 25 °C, 24 h; (c) Boron trifluoroetherate, acetic anhydride, DCM.

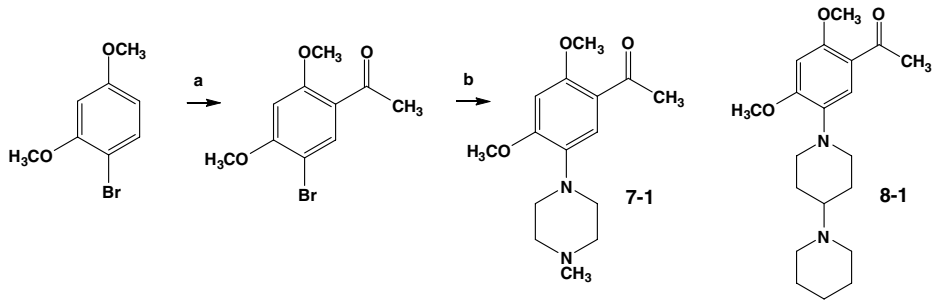

Figure 4. Reagents and conditions: (a) boron trifluoroetherate, acetic anhydride, DCM; (b) $Pd_2(dba)_3$, Cs_2CO_3, rac-BINAP, toluene, reflux, 10 h, 1-methylpiperazine (to give **7-1**) or 1,4′-bipiperidine (to give **8-1**).

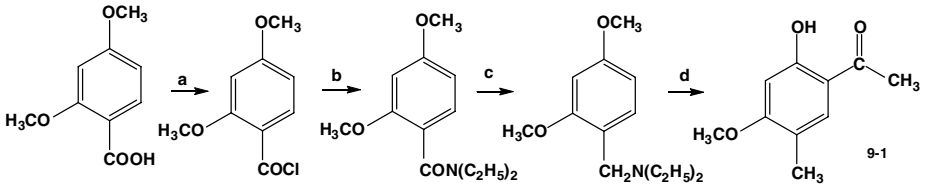

Figure 5. Reagents and conditions: (a) dry benzene, $SOCl_2$, reflux, 2 h; (b) dry THF, diethylamine; (c) borane, dry THF; (d) boron trifluoroetherate, acetic anhydride, DCM.

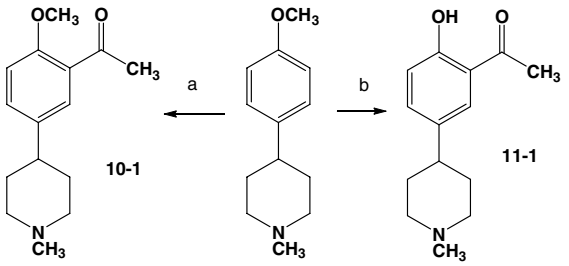

Figure 6. Reagents and conditions: (a) boron trifluoroetherate, acetic anhydride, DCM; (b) $AlCl_3$, acetyl chloride, DCM.

transformed human colon cancer cells HCT 116) and normal human diploid embryonic lung fibroblasts CCL 186. Selectivity ratios ($IC_{50\,CCL186}/IC_{50\,MCF7}$ and $IC_{50\,CCL186}/IC_{50\,HCT}$) were calculated from mean values for each compound. Arbitrary thresholds of $IC_{50} \leqslant 10\ \mu M$ and ratio $\geqslant 2.5$ were used to identify promising compounds. Nearly 2/3rd of the compounds were found to have IC_{50} values that were not significantly greater than 10 μM (independent samples *t*-test, $p < 0.05$). In terms of selectivity ratios, more compounds had selectivity ratios $\geqslant 2.5$ when evaluated against MCF 7 cells (**13**) than HCT 116 cells (**6**).

The contribution of the basic groups to antiproliferative activity was assessed by making the following comparisons which are depicted in Figure 7. First, we compared the activities (based on $IC_{50\,HCT116}$ values) of the non-basic chalcones **5-14**, **5-15**, **5-16** with their counterparts in Groups 1, 6, 7, and 8 (basic group on ring A) (Step A). There was no significant difference in IC_{50} between the non-basic chalcone and its Group 1 or 6 analog, but the Group 7 chalcones (**7-140**, **7-142**) were less active than the non-basic chalcones (**5-15**, **5-16**). This shows that the nature of the basic group on ring A was important in determining the effect on activity. Selectivities were similarly affected as seen from the large falls in selectivities in some groups (7 and 8) and the absence of a specific trend in other groups (1 and 6). The basic group could be introduced into ring B, as shown in Step B of Figure 7. The lone example (**5-16** and **5-113**) showed a fall in activity but more examples would be needed to establish a trend.

Second, comparisons were made to determine if having more than one basic entity made a difference to activity. Only a few compounds were available for this comparison (Step C of Fig. 7), namely, those with basic groups on both rings (**1-123**, **2-124**, **6-134**, and **7-143**) and their counterparts with only a basic group on ring A (**1-6**, **2-3**, **6-131**, and **7-142**). These compounds are listed in Table 2. We found that in 5 out of 8 cases, chalcones with basic groups on both rings had significantly higher IC_{50}values (poorer activity) than those with a single basic group on ring A. No clear trend was observed for selectivity ratios. Step D shows another approach which was to start with compound **5-113**, a monobasic chalcone with the basic moiety on ring B (not ring A) and to compare it with the dibasic chalcones **1-123**, **6-134**, and **7-143** (Table 2). Of the six comparisons made on two cell lines, the IC_{50} values of five were not significantly different from **5-113** but there were more instances (4 out of 6) of a fall in selectivity on going from **5-113** to the dibasic chalcone.

Thus, the nature of the basic group and where it was located (ring A or B) determined its effect on antiproliferative activity. As shown above, 1-methylpiperidine and 1-ethylpiperidine on ring A maintained IC_{50} values while others like 1-methylpiperazine adversely affected activity. In terms of IC_{50} values, there was little advantage in having basic groups on both rings of the chalcone. Based on the limited compound pairs listed in

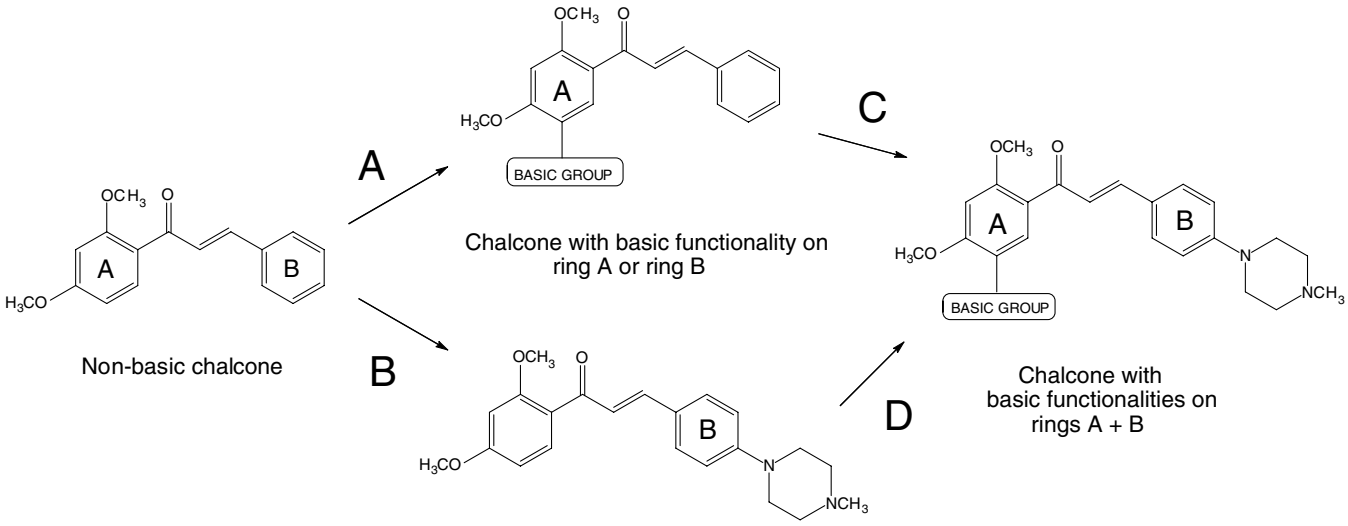

Figure 7. Scheme to summarize effects of basic groups on chalcone rings A and B. Step A: introducing a basic functionality resulted in either no change or a fall in antiproliferative activity, depending on the nature of the basic group. Step B: comparing **5-16** and **5-113** showed a fall in activity. More examples are needed for confirmation. Step C: most examples showed a significant drop in activity and no clear-cut effect on selectivity ratios. Step D: most examples showed no significant change in antiproliferative activity and decrease in selectivity ratios.

Table 2. IC_{50} and selectivity ratios (SR) of chalcones selected to show relative contributions of the basic group to activity and selectivity

Compound	Basic group on ring A[a]	Basic group on ring B[b]	$IC_{50\,MCF7}$ (μM)	$IC_{50\,HCT116}$ (μM)	SR_{MCF7}[c]	SR_{HCT116}[c]
5-113	None	4′-MPZ	13.7 ± 1.8	17 ± 4.6	3.3	2.6
1-123	MP	4′-MPZ	8.5 ± 1.9	7.8 ± 1.8	2.7	2.9
1-6	MP	None	3.4 ± 0.7[d]	2.9 ± 0.5	2.3	2.0
6-134	EP	4′-MPZ	8.8 ± 3.5	10.0 ± 2.7	2.3	2.0
6-131	EP	None	4.8 ± 1.4	7.7 ± 1.6	3.7	2.3
7-143	MPZ	4′-MPZ	13.8 ± 2.4	40.4 ± 6.1[e]	3.4	1.2
7-142	MPZ	None	6.0 ± 1.4[d]	19.4 ± 2.0[d]	2.6	0.8
2-124	MP	4′-MPZ	14.4 ± 1.4	13.9 ± 1.6	0.7	0.7
2-3	MP	None	5.7 ± 1.1[d]	4.2 ± 1.6[d]	1.3	1.7

[a] Structures of compounds are given in Table 1. MP, 1-methylpiperidin-4-yl; EP, 1-ethylpiperidin-4-yl; MPZ, 4-methylpiperazin-1-yl.
[b] 4′-MPZ = 4′-(4-methylpiperazin-1-yl).
[c] SR = Selectivity ratios ($IC_{50\,normal\ cell}/IC_{50\,cancer\ cell}$). Collated from Table 1.
[d] Significant difference between members of same Group (e.g., **1-123** and **1-6**). Independent samples *t*-test, $p < 0.05$. For Step C of Figure 7.
[e] Significantly different from **5-113** (Independent samples *t*-test, $p < 0.05$). For Step D of Figure 7.

Table 2, monobasic chalcones fared better than their dibasic counterparts in terms of IC_{50} values. It was also more advantageous to have the basic moiety on ring A than on ring B, but a basic group on ring B may be better for selectivity. More examples are required to confirm the latter. Interesting, in spite of these general conclusions, the only compound to comply with the threshold limits for IC_{50} and selectivity on both cell lines was the dibasic chalcone **1-123** with 1-methylpiperidinyl on ring A and 4-methylpiperazinyl on ring B. This compound had IC_{50} values of 7.8–8.5 μM and good selectivities (>2.5) for the cancer cell lines. Its Group 6 analog **(6-134)** had comparable activity but poorer selectivity, while its Group 2 and 7 analogs fared poorly in comparison.

3.2. Quantitative structure–activity analysis

Qualitative comparisons like those described in Section 3.1 are generally useful when applied to a small number of compounds but become untenable when analyzing larger libraries. Moreover, such comparisons do not give insight as to why certain variations were observed. A QSAR analysis would provide a better understanding and this approach was adopted here. The compounds were drawn in their predominant ionized forms at pH 7.0 and a range of descriptors were determined in silico from their minimized low energy conformations. The parameters were shape descriptors (molecular length, depth, and width), topological indices (various connectivity and shape indices), steric parameters (area, volume), polarity measures (polar surface area, polar volume, % hydrophilicity, partial positive and negative surface areas), hydrogen bonding parameters (hydrogen bond acceptors and donors, Hansen hydrogen bonding), electronic parameters (molar refractivity, dipole moment, HOMO, LUMO, charge on the α and β carbons on the enone linker), and lipophilicity descriptors (Clog *P*, CNDO log *P*, Crippen log *P*). They are tabulated in Supplementary Information Table 1. Projection methods (principal component analysis PCA and its regression extension, projection to latent structures by

partial least squares analysis PLS)[6] and multiple linear regression (MLR) with stepwise removal of correlated parameters were employed in the analyses.

3.2.1. Projection methods. We found a high degree of correlation among the descriptors. Nearly 50% of the parameters correlated at the level of $r \geqslant 0.75$.[9] Pearson's correlation coefficients for all descriptors are given in Table 2 of Supplementary Information. In view of the high level of correlation, this database would be well suited for analysis by projection methods.[10] The 29 descriptors were first analyzed by principal component analysis (PCA) to reduce them to relevant components that represent the main variations in the data set. A significant two-component model (Model 1) was obtained, with cumulative r^2 (reflecting variability) and cumulative q^2 (reflecting level of predictability) of 0.67 and 0.61, respectively. The 1st component summarized the topological and size parameters, whereas the 2nd component had inputs from lipophilicity and hydrogen bonding parameters. The score plot showed the distribution of the test compounds based on these components (Fig. 8) and it revealed distinct clustering among certain Groups. These were Groups 1, 7 that had different basic groups on ring A, and Groups 5, 9 that had no basic group on ring A. This implied that the clustered groups shared similar physicochemical profiles and were different from the non-clustered groups. It would be advisable to analyze their QSAR separately from other groups. Fig. 8 also showed that some members in Groups 1, 2, 6, and 7 were isolated from the other compounds in the group. Interestingly, all the outlying compounds were found to have a 1-methylpiperazine group on ring B.

PLS is a regression extension of principal component analysis. In PLS, principal components are calculated to explain most of the variance in the descriptor set and to concurrently maximize their correlations with the dependent variable.[10] In spite of the clustering of certain groups in the score plot (Fig. 8), PLS was applied to the entire library of compounds. This decision was made because the PLS models derived from the clustered groups (not shown) did not give additional insight into SAR, although they were statistically more robust. In addition, the small number of compounds in the clustered groups may lead to over-interpretation of the SAR trends.

A PLS model was obtained by the regression of the combined pIC_{50} values of the compounds against the descriptor set. A significant two-component model (Model 2) with satisfactory cumulative r^2 (0.443) and q^2 (0.283) was obtained. The loadings plot (Fig. 9) showed that the two pIC_{50} values were close but did not overlap. Thus, these values could be modeled separately. Figure 9 also showed that the IC_{50} values were largely influenced by the same parameters: a large dipole moment and polar volume coupled with an electron poor β carbon were favourable for activity, whereas the presence of hydrogen bonding groups and a large (more negative) HOMO energy had an inverse effect on activity. When PLS was applied to the selectivity ratios as dependent variables, no significant model was obtained (r^2 (0.082), q^2 (0.032)).

In view of the good outcome of Model 2, PLS for each pIC_{50} was separately determined and the model statistics summarized in Table 3. It was noted that a statistically more robust PLS model was obtained with $pIC_{50\,MCF7}$ (Model 4) than $pIC_{50\,HCT116}$ (Model 3). Polar volume, HOMO, and the charge on β carbon were important parameters influencing both activities. Dipole moment strongly influenced $pIC_{50\,HCT116}$ but was not among the top four descriptors for Model 4 ($pIC_{50\,MCF7}$). H donor properties were rated prominently for $pIC_{50\,MCF7}$ but not for $pIC_{50\,HCT116}$. Some comments on these parameters are given in the following paragraphs.

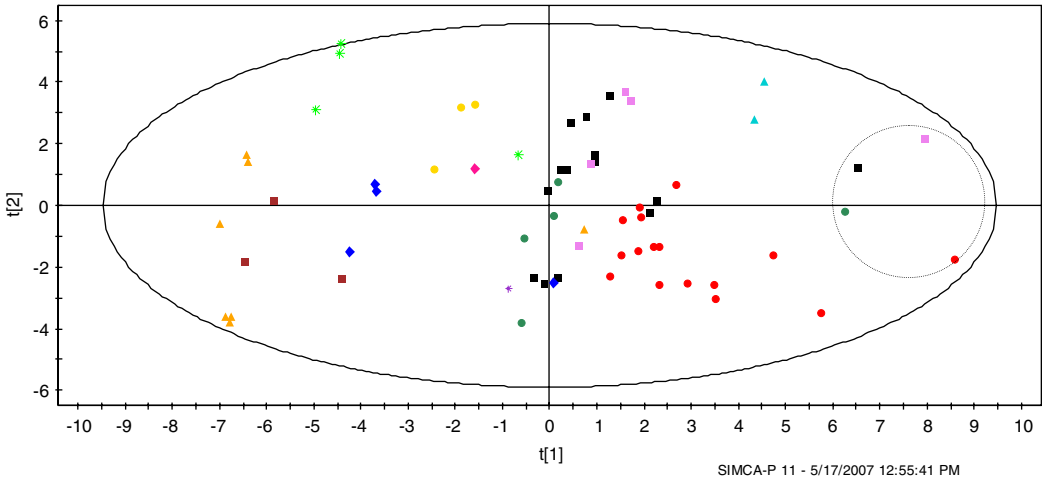

Figure 8. PCA score plot of $t[1]$ (1st principal component) versus $t[2]$ (2nd principal component) for chalcones ($n = 65$, 29 descriptors). Group (G) 1, black □; G2, red ○; G3, blue ◇; G4, green ∗; G5, yellow △; G6, pink □; G7, green ○; G8, blue △; G9, brown □; G10, yellow ◇; G11, red ◇; Compound **13**, purple ◇. G5 (yellow △) and G9 (brown □) do not have basic groups on ring A and are clustered on the left of quadrant. G1 (black □) and G7 (green ○) are also clustered along the midline. Outliers in G1, G2, G6 and G7 are enclosed in circle on right quadrant. These outliers are **1-123**, **2-124**, **6-134**, **7-143**. The eclipse corresponds to the confidence region based on Hotelling T^2 (0.05).

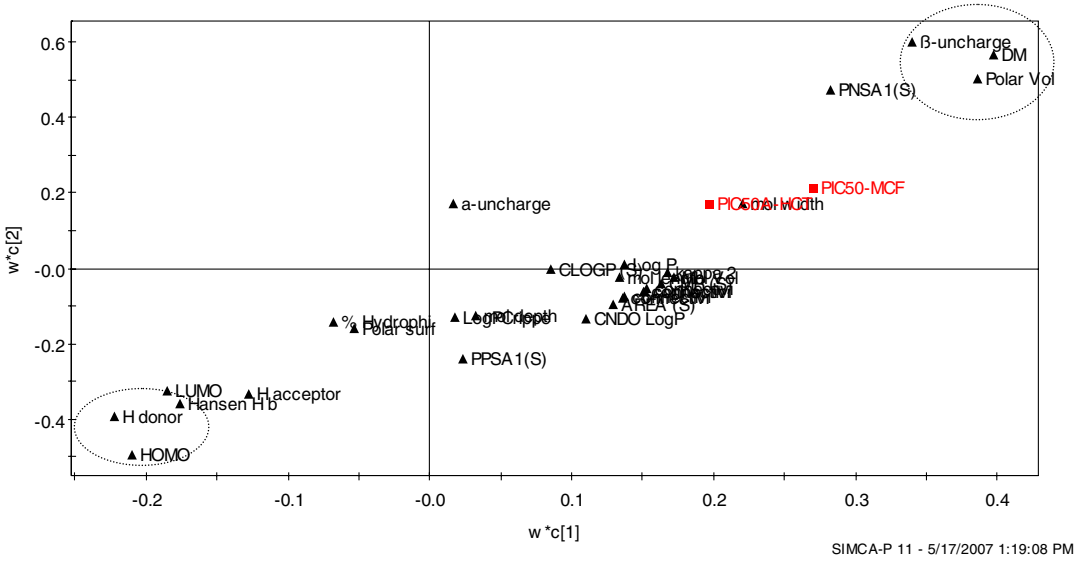

Figure 9. PLS Loading plot for $pIC_{50\,MCF}$ (n = 61, 29 descriptors) and $pIC_{50\,HCT}$ (n = 65, 29 descriptors). Parameters that were displaced far away from origin contributed significantly to activity. The important contributors (encircled) were dipole moment DM, charge on β carbon (β uncharged), polar volume (top right quadrant), and HOMO, H donor (lower left quadrant).

Polar volume was identified in both Models 3 and 4 as an important factor directly influencing antiproliferative activity. When the polar volumes of the various groups were examined, a general trend was that chalcones with more substituents on ring A had larger polar volumes. This is shown in Table 4 where compounds from different groups but with the same ring B substituent (2′-Cl in this case) were compared. Polar volume was largest for the highly substituted Group 2 compound (**2-17**) and decreased as substituents on ring A were progressively removed. Thus polar volume decreased in the order **2-17** > **1-5** > **10-8** > **11-11**. However, IC_{50} of these compounds did not always change in the expected manner, suggesting that other factors besides polar volume contributed to the final activity profile. Besides the degree of substitution on ring A, within each group, larger polar volumes were found in compounds with 4-methylpiperazin-1-yl and dimethylamino groups on ring B. Pyridine as ring B was also associated with a larger polar volume than the phenyl ring B. For example, the polar volume of **1-6** (no substituent on ring B, 387 Å^3) increased to 431 Å^3 (**1-123**) and 535 Å^3 (**1-121**) on substitution with 4′-(4-methylpiperazin-1-yl) and 3′-pyridinyl (in place of ring B), respectively. As before, an increase in polar volume was not always accompanied by greater activity.

Dipole moment was identified as an important contributor to $pIC_{50\,HCT116}$ but not $pIC_{50\,MCF7}$. Since dipole moment and polar volume were significantly correlated to each other (Pearson's correlation coefficient r = 0.387, p 0.001, two-tailed), this difference may not be important. Interestingly, within each group, compounds with 2′-Cl or 2′-F on ring B had larger dipole moments than compounds with 4′-Cl or 2′-OCH_3.

The β carbon of all the compounds had a positive charge when evaluated in their non-protonated states. This is due to the transmission of the electron withdrawing effect of the carbonyl oxygen. A more electron deficient β carbon was associated with better activity (Models 3 and 4, Table 3), which was in keeping with proposal by Dimmock et al.[3] The magnitude of the positive charge on the β carbon varied with the nature of ring B and was generally greater than 0.04 esu (Table 2, Supplementary Information). One notable exception was when ring B had a 4′-(4-methylpiperazin-1-yl) substituent, which caused the positive charge on the β carbon to be reduced to 0.031–0.037 esu. This may be due to the aniline-like character of the proximal nitrogen atom of the piperazine ring. The lone pair of electrons on the proximal nitrogen were delocalized into ring B and this may lead to the reduction in positive charge.

The PLS models identified low (more negative) HOMO energies and poor H bonding capabilities as important factors for good antiproliferative activity. The HOMO energies were strongly influenced by the substitution pattern on rings A and B. In particular, electron withdrawing groups (F, Cl, CF_3, pyridine) on ring B resulted in low (favorable) HOMO energies while electron donating groups on ring B like 4′-dimethylamino and 4′-(4-methylpiperazin-1-yl) had the opposite (unfavorable) effect. H bond donor capability was identified as an undesirable feature affecting $pIC_{50\,MCF7}$ (Model 4), but not $pIC_{50\,HCT116}$ (Model 3). This difference may not be important as there were significant correlations among the parameters. HOMO and H bond acceptor were correlated at $p < 0.01$ (r = 0.324, two-tailed). Similarly, the descriptors H bond acceptor and H bond donor were correlated (r = 0.761, $p < 0.01$, two-tailed). Hence, we concluded that both pIC_{50} values were adversely affected by H bonding features. These features were most prominent for Groups 2 and 9 that had the OH group on ring A. Thus, several members in these groups had poor pIC_{50} values.

As stated earlier, the key parameters interacted with each other to influence the final activity of the com-

Table 3. Summary of model statistics from PLS and MLR

Model 3 (projection method, PLS)[a]
Dependent variable: $pIC_{50\,HCT116}$
Number of components: 3
Cumulative r^2 0.49
Cumulative q^2 0.23
Top four descriptors contributing to activity[c]
Dipole moment (+), polar volume (+), HOMO (−), charge on β carbon (+)
Model 4 (projection method, PLS)[a]
Dependent variable: $pIC_{50\,MCF7}$
Number of components: 3
Cumulative r^2 0.66
Cumulative q^2 0.50
Top four descriptors contributing to activity[c]
Charge on β carbon (+); HOMO (−); Polar Volume (+); H bond donor (−)
Model 5 (MLR, stepwise)[b]
Dependent variable: $pIC_{50\,HCT116}$
r^2 0.27
F 11.49
Standard error of estimate 0.32
Descriptors[c]: dipole moment (+), H bond donor (−)
Model 6 (MLR, stepwise)[b]
Dependent variable: $pIC_{50\,MCF7}$ r^2 0.42
F 22.74
Standard error of estimate 0.28
Descriptors[c] polar volume (+), H bond acceptor (−)
Model 7 (MLR, stepwise)[b]
Dependent variable: selectivity ratio against MCF 7 cells (SR_{MCF7})
r^2 0.49
F 55.78
Standard error of estimate 0.64
Descriptor: H bond donor (−)

[a] PLS models were obtained with Simca-P 11.0, Umetrics (Umea, Sweden).

[b] Multiple linear regression (MLR) with stepwise omission of parameters were run on SPSS for Windows, Version 14.0 (Chicago, IL).

[c] Descriptors are cited in order of decreasing contribution to model. (+) Directly correlated to activity; (−) Inversely correlated to activity.

pound. The following two examples served to illustrate this point. Compound **10-8** had good activity against HCT 116 cells (IC_{50} 2.3 μM). It had a 2′-Cl substituent on ring B and its ring A was substituted with 2-methoxy and 5-(1-methylpiperidin-4-yl). It had the necessary attributes for good activity, namely, a large dipole moment, low HOMO energy, and reasonable electron deficiency at the β carbon. These properties were traced to the presence of the electron withdrawing 2′-Cl on ring B. On the other hand, it had a small polar volume because of the ring A substitution pattern but this deficiency was adequately compensated by other advantageous features (dipole moment, HOMO, charge on β carbon). Another example is compound **2-17** which had IC_{50} values of 3 μM against both cell lines. Compound **2-17** had 2′-Cl on ring B and ring A substituted with two methoxy groups, 1-methylpiperidine and a phenolic OH. In this case, good activity was retained in spite of the H bonding features of the phenolic OH. It may have been compensated in part by the favorable HOMO energy and electron deficiency at the β carbon (due to the electron withdrawing 2′-Cl on ring B) and its large polar volume (highly substituted ring A).

3.2.2. Multiple linear regression. Besides projection methods, multiple linear regression (MLR) with stepwise elimination of correlated parameters was also employed for model construction. The results are summarized in Table 3. MLR gave rise to models with poorer r^2 values but shared several similarities to the PLS models. As before, better model statistics were observed with $pIC_{50\,MCF7}$ as compared to $pIC_{50\,HCT116}$. In addition, the critical parameters identified by MLR coincided to some extent with those found for the projection methods. In the case of $pIC_{50\,MCF7}$, polar volume and H bonding were ranked highly by both methods. For $pIC_{50\,HCF116}$, both methods highlighted the contribution of dipole moment, but H bond donor was identified by MLR (not PLS) as an important feature.

As mentioned earlier, projection methods failed to identify statistically significant models for selectivity ratios against HCT (SR_{HCT}) and MCF (SR_{MCF}). MLR did not give a credible model for SR_{HCT}, but a fairly promising model was obtained for SR_{MCF} (Model 7, Table 3). In this model, the presence of H bond donors was identified as the only factor that adversely affected selective activity. This is an interesting finding because it implied that omitting or reducing the presence of H bond donors in compounds may lead to good activity and selectivity against MCF 7 cells.

3.3. Effect of selected chalcones on cell cycle of HCT 116 cells

We showed previously that compound **1-5** at 5 μM, a concentration close to its IC_{50}, caused HCT16 cells to be arrested at the G1 phase, but not at the G2/M phase.[4]

Table 4. Polar volumes of representative chalcones with 2′-Cl on ring B

Compound[a]	IC_{50}[b] (μM)	Polar volume[c] (Å^3)	Compound[a]	IC_{50}[b] (μM)	Polar volume[c] (Å^3)
1-5	2.8, 3.4	331.6	**7-140**	6.2, 14.1	361.6
2-17	3.1, 3.1	495.1	**8-160**	3.7, 19.3	333.2
3-101	21.4, 10.5	132.7	**9-150**	22.4, 43.9	45.9
4-104	47.4, 23.9	33.1	**10-8**	2.9, 2.3	289.2
5-15	ND, 5.2	296.8	**11-11**	ND, 6.9	255.1
6-130	2.6, 6.7	369.2			

[a] Structures of compounds are given in Table 1.

[b] The two values are the $IC_{50\,MCF7}$ and $IC_{50\,HCT116}$, cited in that order. ND, not determined.

[c] Polar volume was determined from Sybyl 7.0 (Tripos Associates, St. Louis, MO).

At higher concentrations (10 and 20 μM), both phases of the cell cycle were affected. We also found that compounds **5-14** and **13**, with no basic moieties on ring A, did not affect the cell cycle at concentrations close to their IC_{50} values.[4] This led us to propose that the presence of a basic group played a special role in targeting the G1 phase of the cell cycle. To test our hypothesis, we extended our investigations to three analogs of compound **1-5**, namely **1-123**, **6-130**, and **7-140**. Compound **1-123** had 4-methylpiperazin-1-yl on ring B and 1-methylpiperidin-4-yl on ring A and was identified as a promising compound based on its IC_{50} and selectivity profile. Compounds **6-130** ($IC_{50\,HCT116}$ 6.7 μM) and **7-140** ($IC_{50\,HCT116}$ 14.1 μM) had 1-ethylpiperidin-4-yl and 4-methylpiperazin-1-yl groups on ring A, respectively. Both compounds had in common 2'-Cl on ring B. The three compounds were tested at 5 and 0.5 μM for their ability to interfere with the transition of HCT 116 cells from G1 to G2/M, as well as cells released from a G2/M block and moving on to G1. The results are summarized in Table 5.

The cell cycle progression experiments were designed to examine synchronized cell populations at G1 or G2/M phase though one transit of the cell cycle. When cells were arrested at the G1 phase, the proportion of G1 cells, 24 h after their release from G1 block, would remain high and there would be fewer cells in the G2/M phase. When cells were arrested at the G2/M phase, the proportion of cells in this phase, 6–8 h after their release from the G2/M block, would remain high, and there would be few cells in the G1 phase.

Based on these criteria, compound **1-123** did not cause G1 arrest or G2 arrest at 5 and 0.5 μM. The proportion of cells in G1 and G2/M were quite similar to that of control (untreated) cells in each case. On the other hand, compound **6-130** arrested cells at both G1 and G2/M phases at 5 μM but not at 0.5 μM. It caused a sharp rise in cells at the G1 phase (65% compared to 35% for control cells, Table 5A). In its presence, the proportion of cells at the G2/M phase was 47%, compared to 32% for control cells (Table 5B). In the case of compound **7-140**, it arrested the cells at the G1 phase only at 5 μM (52% compared to 35% for control cells, Table 5A). It had no effect on cells released from G2/M block.

The results showed that changing the ring A basic group affected the phase of the cell cycle transition that was interrupted. Compounds **1-5** and **7-140** only interfered with the G1 phase, suggesting that the 1-methylpiperidinyl and 4-methylpiperazinyl groups had equivalent effects. In contrast, changing the 1-methylpiperidinyl ring of **1-5** to 1-ethylpiperidinyl ring (**6-130**) caused both G1 and G2/M phases to be affected. Despite its good activity and selectivity, **1-123** did not interfere with the cell cycle, indicating that an extra basic group on ring B had a significant effect on the mechanism of action. Our preliminary results showed that **1-123** did not interfere with tubulin binding which was an effect widely associated with antiproliferative chalcones.[11] Further investigations into its mode of action are in progress. The score plot (Fig. 8) showed that dibasic chalcones like **1-123** were outliers from their respective groups. Interesting, **1-123** had no effect on the cell cycle, in con-

Table 5. Effect of chalcones **1-123**, **6-130**, and **7-140** on distribution of HCT 116 cells in various phases of the cell cycle

Time (h)[b]	Concentration (μM)	**1-123**[c]			**6-130**[c]			**7-140**[c]		
		G_1	S	G_2/M	G_1	S	G_2/M	G_1	S	G_2/M
(A) Cells released from G1 block[a]										
8	5	69.4 (65.6)	3.6 (3.5)	27.1 (30.7)	70.7 (65.6)	3.2 (3.5)	26.1 (30.7)	65.3 (65.6)	3.8 (3.5)	30.8 (30.7)
24		49.4 (35.1)	18.7 (16.7)	33.4 (49.1)	65.0 (35.1)	6.4 (16.7)	28.8 (49.1)	52.2 (35.1)	17.5 (16.7)	31.7 (49.1)
48		52.4 (59.0)	12.8 (7.7)	35.6 (34.0)	59.4 (59.0)	6.8 (7.7)	32.8 (34.0)	63.4 (59.0)	6.5 (7.7)	30.1 (34.0)
8	0.5	68.2 (65.6)	3.6 (3.5)	28.3 (30.7)	66.3 (65.6)	3.6 (3.5)	30.2 (30.7)	68.9 (65.6)	3.3 (3.5)	27.8 (30.7)
24		36.6 (35.1)	16.5 (16.7)	47.9 (49.1)	34.1 (35.1)	18.2 (16.7)	49.3 (49.1)	35.6 (35.1)	18.2 (16.7)	47.6 (49.1)
48		58.2 (59.0)	9.0 (7.7)	33.2 (34.0)	59.9 (59.0)	8.9 (7.7)	31.8 (34.0)	59.9 (59.0)	7.4 (7.7)	33.3 (34.0)
(B) Cells released from G_2/M block[d]										
Time (h)[e]	Concentration (μM)	**1-123**[c]			**6-130**[c]			**7-140**[c]		
		G_1	S	G_2/M	G_1	S	G_2/M	G_1	S	G_2/M
6	5	55.9 (59.5)	10.0 (9.2)	34.9 (32.3)	45.3 (59.5)	8.2 (9.2)	47.1 (32.3)	53.2 (59.5)	9.0 (9.2)	38.7 (32.3)
24		53.7 (59.0)	8.0 (7.7)	38.7 (34.0)	50.7 (59.0)	9.9 (7.7)	39.8 (34.0)	54.3 (59.0)	7.1 (7.7)	38.8 (34.0)
48		54.5 (63.9)	8.5 (5.3)	37.3 (30.7)	63.0 (63.9)	4.9 (5.3)	32.0 (30.7)	59.2 (63.9)	4.3 (5.3)	34.6 (30.7)
6	0.5	53.9 (59.5)	12.7 (9.2)	34.6 (32.3)	51.4 (59.5)	12.5 (9.2)	36.9 (32.3)	54.2 (59.5)	11.6 (9.2)	35.2 (32.3)
24		50.9 (59.0)	8.2 (7.7)	41.2 (34.0)	53.8 (59.0)	9.1 (7.7)	37.6 (34.0)	53.8 (59.0)	7.3 (7.7)	39.2 (34.0)
48		54.8 (63.9)	10.8 (5.3)	34.2 (30.7)	50.5 (63.9)	5.5 (5.3)	43.9 (30.7)	56.5 (63.9)	4.6 (5.3)	38.4 (30.7)

[a] Proportion of cells at start of experiment (0 h) were G_1 59.9; S 3.4; G_2/M 35.6.

[b] Time (h) after cells were released from the G_1 block. Proportion of cells at the 24-h time point would indicate if test compound blocked G1 → G2 phase transition.

[c] % Cells in each phase after exposure to test compound at the stated concentration. Values in parentheses represent control values in concurrent experiments.

[d] Proportion of cells at start of experiment (0 h) were G_1, 35.1; S, 16.7; G_2/M, 49.1.

[e] Time (h) after cells were released from G_2/M block. Proportion of cells at the 6-h time point would indicate if test compound blocked G2 → G1 phase transition.

trast to another compound in the same group (**1-5**) which was shown in an earlier study[4] to cause arrest of the G1 phase of proliferating HCT 116 cells.

4. Conclusion

The objective of this study was to evaluate the SAR of the antiproliferative activity of chalcones and to determine if the critical factors that affected activity were influenced by the basic group(s) in the chalcone template. QSAR analyses identified four parameters as major contributors to activity, namely polar volume, H bonding features, HOMO energies, and charge on β carbon. Good antiproliferative activity was associated with large polar volumes, the absence of H bonding groups, low HOMO energies, and an electron deficient β carbon. The basic group contributed to a desirable increase in polar volume but adversely affected HOMO and charge on β carbon when located on ring B. It did not significantly affect H bonding parameters. Thus the final activity profile of the basic chalcone depended on a close interplay among these factors.

The nature of the basic entity was also important. In general, chalcones with a single basic functionality had better antiproliferative activities than those with more than one basic group. It was also preferable to locate the basic entity on ring A rather than ring B. In spite of these generalizations, the most promising compound in the library was a dibasic chalcone (**1-123**) which had 1-methylpiperidinyl on ring A and 4-methylpiperazinyl on ring B. Finally, it was noted that that structural differences in the chalcones also influenced their downstream effects. Compounds **1-5**,[4] **6-130**, and **7-140**, characterized by a single basic entity on ring A, arrested the cell cycle at either G1 or G1 and G2/M phases. On the other hand, compound **1-123** with two basic groups did not interfere with the cell cycle. Thus a different mechanism accounted for its good antiproliferative activity.

5. Experimental

5.1. Chemistry

Melting points were determined in open glass capillary tubes on a Gallenkamp melting point apparatus and were uncorrected. ^{1}H NMR and ^{13}C NMR spectra were recorded on a Bruker DPX 300 MHz spectrometer and chemical shifts were reported in δ (ppm) relative to the internal standard TMS. Mass spectra were collected on LcQ Finnigan MAT mass spectrometer with chemical ionization (APCI) or electron spray ionization (ESI) as probes. Analytical thin-layer chromatography was performed on TLC silica gel 60 F_{254} (230–400 mesh) and MKC18F silica gel 60 plates (size 2.5 × 7.5 cm). Preparative MPLC was done using a C_{18} column (Merck Lichropret RP-18, 15–25 μm) on a Shimadzu Prominence instrument. The purity of the final compound was confirmed by reverse-phase HPLC (X-Bridge C-18, 150 mm × 3.0 mm, 3 μM particle size) using two mobile phases, methanol–water and acetonitrile–water.

5.1.1. General procedure for the synthesis of chalcones.[4] A solution of the aldehyde (1.2 mmol) in methanol (5 ml) was added dropwise to a stirred solution of the acetophenone (1 mmol) dissolved in 3% (w/v) NaOH in methanol (20 ml). The solution was stirred at room temperature (28 °C) for 12 h. Alternatively, the reagents were reacted under microwave at 130 °C, 3 min in a Biotage Initiator™ (Biotage AB, Uppsala, Sweden) microwave reactor. The solvent was removed under reduced pressure. The resulting residue was dissolved in 1 M HCl and extracted with ether. The aqueous layer was rendered alkaline with saturated aqueous Na_2CO_3 solution to give a precipitate that was filtered, washed with water, and dried. Some products were obtained by recrystallization from methanol–water, whereas others were purified by MPLC. Yields, mp, NMR chemical shifts, and MS data of synthesized chalcones are given in Supplementary Information, Appendix 1.

5.1.2. Syntheses of acetophenones. Syntheses of **1-1**, **1-2**, and **1-10** were described earlier.[4] 1-(4-Piperazin-1-yl-phenyl)ethanone and 1-(4-piperidin-1-yl-phenyl)ethanone, starting acetophenones for Groups 3 and 4, were purchased from Sigma–Aldrich Corporation (St. Louis, Missouri, USA).

5.1.2.1. 1-Ethyl-4-(2,4-dimethoxyphenyl)-1,2,3,6-tetrahydropyridine. 1-Ethylpiperidin-4-one (0.15 mol) was added to a stirred solution of 1,3,5-trimethoxybenzene (0.15 mol) in glacial acetic acid (200 ml) at 15–20 °C. HCl gas was bubbled through the reaction mixture (1 h), followed by stirring at rt 24 h, and heating for 3 h at 95–100 °C. The solvent was removed under reduced pressure and the residue was diluted with water. The aqueous solution was extracted with ether and the aqueous layer made alkaline with 1 M NaOH. The crude product was extracted with ethyl acetate and purified by flash column. Yield: 65%. MS-APCI: $[M+H]^+$ 248.2 (247.2). ^{1}H NMR ($CDCl_3$): 7.10–7.07 (1H, mb), 6.45–6.43 (2H, mb), 5.74 (1H, mb), 3.80 (3H, s), 3.78 (3H, s), 3.13–3.12 (2H, m), 2.68–2.51 (6H, m), 1.18–1.13 (3H, t). ^{13}C NMR ($CDCl_3$): 159.8, 157.8, 135.1, 129.8, 124.7, 123.3, 103.9, 98.7, 55.3, 52.8, 52.2, 50.1, 29.7, 12.2.

5.1.2.2. 1-Ethyl-4-(2,4-dimethoxyphenyl)-piperidine. 1-Ethyl-4-(2,4-dimethoxyphenyl)-1,2,3,6-tetrahydropyridine (5 g) was hydrogenated in acetic acid/water (10:1, 150 ml) with 10% palladium on carbon (0.5 g) as catalyst at 30–40 psi, rt, 24 h. The reaction mixture was filtered over Celite and the solvent removed in vacuo to give a residue which was diluted with water, made alkaline with 1 M NaOH, and extracted with ethyl acetate. The residue left on evaporation of solvent at reduced pressure was a liquid. It was dried under vacuum and used without further purification. Yield: 94%. ^{1}H NMR ($CDCl_3$): 7.13–7.10 (1H, m), 6.47–6.45 (2H, m), 3.799 (3H, s), 3.791 (3H, s), 3.08–3.04 (2H, m), 2.86 (1H, mb), 2.46–2.43 (3H, q), 2.05–2.03 (2H, m), 1.78–1.75 (4H, m), 1.14–1.09 (3H, t). ^{13}C NMR ($CDCl_3$): 158.8, 157.7, 127.0, 126.8, 103.9, 98.5, 55.2, 55.1, 54.2, 52.7, 34.7, 32.3, 12.1.

5.1.2.3. 1-(2,4-Dimethoxy-5-(1-ethylpiperidin-4-yl)phenyl)ethanone (6-1). The procedure for the synthesis of **1-1** was followed as described earlier.[4] **6-1** was obtained in 83% yield after recrystallization from methanol/water (2:1). Mp 128–129 °C, MS-APCI: $[M+H]^+$ 292.5 (291.2). ^1H NMR ($CDCl_3$) 7.75 (1H, s), 6.41 (1H, s), 3.92 (3H, s), 3.89 (3H, s), 3.10–3.07 (2H, m), 2.86–2.77 (1H, mb), 2.56 (3H, s), 2.51–2.44 (2H, q), 2.10–2.02 (2H, m), 1.79–1.71 (4H, m), 1.16–1.11 (3H, t). ^{13}C NMR ($CDCl_3$): 197.6, 161.7, 159.6, 129.4, 126.7, 120.0, 94.4, 55.5, 55.4, 54.1, 52.6, 35.1, 31.9, 31.8, 12.1.

5.1.2.4. 1-(5-Bromo-2,4-dimethoxyphenyl)ethanone. Boron trifluoride dimethyletherate (46 ml, 0.5 mol) was added dropwise to a stirred solution of 1-bromo-2,4-dimethoxybenzene (7.2 ml, 0.05 mol) in CH_2Cl_2 (150 ml) which had been cooled in an ice bath. Acetic anhydride (37.8 ml) was added dropwise to the solution and stirring was continued for 24 h at room temperature. The reaction mixture was diluted with water, rendered alkaline with Na_2CO_3, and extracted with CH_2Cl_2. Removal of solvent in vacuo gave a solid residue that was recrystallized with ethyl acetate/hexane to give the product in 85% yield. Mp 149–150 °C. MS-APCI: $[M+H]^+$ 259.5:261.2 (1:1) (258.0). ^1H NMR ($CDCl_3$): 8.04 (1H, s), 6.45 (1H, s), 3.96 (3H, s), 3.94 (3H, s), 2.56 (3H, s). ^{13}C NMR ($CDCl_3$): 196.3, 160.4, 160.0, 135.1, 121.4, 102.7, 95.7, 56.3, 55.7, 31.7.

5.1.2.5. 1-[2,4-Dimethoxy-5-(4-methylpiperazin-1-yl)phenyl]ethanone (7-1). Cesium carbonate (1.4 equiv) was finely ground in a nitrogen-filled glovebox and weighed into an oven-dried Schlenk flask. The flask was quickly capped with a rubber septum and purged with argon. Pd_2 $(DBA)_3$ (tris(dibenzylidene acetone)dipalladium (0), 0.0025 mmol, 0.5% Pd) and rac-BINAP (rac-2,2′-bis(diphenylphosphino)-1,1′-binaphthyl) (0.0075 mmol) were added into the flask, followed by 1-(5-bromo-2,4-dimethoxyphenyl)ethanone (1.0 mmol), 1-methylpiperazine (1.1–1.2 mmol), and toluene (4 ml). The flask was immersed in an oil bath (100 °C), stirred for 10 h until the starting materials had been completely consumed as judged by TLC. The solution was then cooled to room temperature, diluted with ether, filtered, and concentrated in vacuo. The crude product was purified by flash chromatography on silica gel to give a yield of 76%. Mp 75–76 °C, MS-APCI $[M+H]^+$: 279.5 (278.2). ^1H NMR ($CDCl_3$): 7.46 (1H, s), 6.44 (1H, s), 3.91 (3H, s), 3.89 (3H, s), 3.03 (4H, br), 2.61 (4H, br), 2.55 (3H, s), 2.33 (3H, s). ^{13}C NMR ($CDCl_3$): 197.5, 157.3, 157.1, 134.6, 120.1, 119.4, 95.8, 55.75, 55.71, 55.1, 50.7, 45.9, 31.9.

5.1.2.6. 1-(2,4-Dimethoxy-5-(4-(piperidin-1-yl)piperidin-1-yl)phenyl)ethanone (8-1). The method for **7-1** was followed using 1,4′ –bipiperidine. Compound **8-1** was obtained in 49% yield, mp 257–258 °C (HCl salt), MS-APCI $[M+H]^+$: 345.2 (346.2). ^1H NMR (MeOD): 8.11 (1H, s), 6.90 (1H, s), 4.12 (3H, s), 4.02 (3H, s), 3.82–1.55 (22H, m). ^{13}C NMR (MeOD): 197.3, 163.1, 157.2, 124.6, 122.2, 120.7, 98.4, 60.5, 58.0, 56.9, 54.1, 51.4, 48.4, 24.9, 23.7, 22.2.

5.1.2.7. 1-(2-Hydroxy-5-(1-methylpiperidin-4-yl)phenyl)-ethanone (11-1). A stirred solution of 4-(4-methoxyphenyl)-1-methylpiperidine[4] (1.8 g) in CH_2Cl_2 (50 ml) was cooled in an ice bath. Powdered $AlCl_3$ (1.8 g) was added in small portions, followed by dropwise addition of acetyl chloride (0.8 ml). Stirring was continued for 24 h at room temperature. The reaction mixture was diluted with water, made alkaline with Na_2CO_3, and extracted with CH_2Cl_2. Removal of solvent in vacuo gave a solid residue that was recrystallized with methanol/water (2:1) to give the desired product in 75% yield. Mp 83–85 °C. ^1H NMR ($CDCl_3$): 12.10 (1H, s, OH), 7.55–7.54 (1H, d, $J = 1.9$ Hz), 7.35–7.32 (1H, dd, $J_1 = 8.6$ Hz, $J_2 = 1.9$ Hz), 6.92–6.89 (1H, d, $J = 8.6$ Hz), 2.99–2.95 (2H, mb), 2.60 (3H, s), 2.45–2.40 (1H, m), 2.32 (3H, s), 2.09–2.01 (2H, m), 1.82–1.74 (4H, m). ^{13}C NMR ($CDCl_3$): 204.4, 160.7, 136.7, 135.4, 128.3, 119.4, 118.3, 56.1, 46.3, 41.1, 33.5, 26.6.

5.1.2.8. *N*,*N*-Diethyl-2,4-dimethoxybenzamide.[8] 2,4-Dimethoxybenzoic acid (3.2 g, 1.8 mmol), thionyl chloride (HAZARD) (7.8 ml), and dry benzene (HAZARD) (100 ml) were heated at reflux under stirring for 2 h. Solvent and excess thionyl chloride were removed under vacuum and the crude acid chloride (3.6 g, 1.8 mmol) was dissolved in benzene (40 ml). This solution was cooled to 0 °C and diethylamine (5.6 ml, 5.4 mmol) in dry THF (15 ml) was added dropwise to the stirred solution. After the addition was completed, the reaction mixture was stirred for 2 h at 0 °C and then for 8 h at room temperature. The solvents were removed under reduced pressure and the residue was extracted with CH_2Cl_2. The organic layer was thoroughly washed with 5% Na_2CO_3, 5% HCl, and water. Removal of solvent after drying the organic layer afforded the product which was used without further purification. ^1H NMR ($CDCl_3$, 300 MHz, δ, ppm): 7.13–7.10 (1H, d, $J = 8.3$ Hz), 6.50–6.44 (2H, m), 3.81 (3H, s), 3.79 (3H, s), 3.53 (2H, br), 3.14 (2H, br), 1.22–1.20 (3H, mb), 1.02 (3H, br).

5.1.2.9. *N*-(2,4-Dimethoxybenzyl)-*N*-ethylethanamine. Borane (1 M solution in THF, 15 ml) in THF (15 ml) was slowly added to a stirred solution of *N*,*N*-diethyl-2,4-dimethoxybenzamide (1.2 g, 5 mmol) in THF (10 ml) in an ice bath. The reaction was stirred for 5 h under an atmosphere of argon followed by dropwise addition of methanol. Evaporation in vacuo followed by addition of 6 M HCl gave a suspension that was stirred for 18 h. The mixture was made alkaline using 2 M NaOH and extracted with ether. The product was used for the next step of the reaction without further purification. ^1H NMR ($CDCl_3$): 7.35–7.33 (1H, d, $J = 8.3$ Hz), 6.50–6.44 (2H, m), 3.96 (2H, s), 3.81 (3H, s), 3.79 (3H, s), 2.75–2.68 (4H, q), 1.28–1.23 (6H, t).

5.1.2.10. 1-(2-Hydroxy-4-methoxy-5-methylphenyl)ethanone (9-1). *N*-(2,4-Dimethoxybenzyl)-*N*-ethylethanamine (0.05 mol) was reacted with boron trifluoride dimethyletherate (0.5 mol) and acetic anhydride (38 ml) in CH_2Cl_2 as described in 5.1.2.2. The product was found to be 9.1, indicating that loss of the diethyl-

amino function and demethylation had occurred during the reaction. Yield: 52%, mp 64–65 °C, MS-APCI $[M+H]^+$: 181.4 (180.1). ^1H NMR ($CDCl_3$): 12.69 (1H, OH), 7.42 (1H, s), 6.38 (1H, s), 3.85 (3H, s), 2.55 (3H, s), 2.14 (3H, s). ^{13}C NMR ($CDCl_3$): 202.4, 164.4, 163.8, 131.7, 118.0, 113.0, 98.8, 55.6, 26.2, 15.5.

5.1.3. Syntheses of benzaldehydes. Only 4′-(4-methylpiperazin-1-yl)benzaldehyde was synthesized. The other benzaldehydes were purchased from commercial sources (Sigma–Aldrich Chemical Company).

5.1.3.1. 2-(4-Bromophenyl)-1,3-dioxane. A solution of 4-bromobenzaldehyde (4.3 g, 23 mmol), 1,3-propanediol (16.8 ml, 0.23 mmol), and *p*-toluenesulphonic acid (0.05 g) in toluene (150 ml) was refluxed for 28 h. Water was removed using a Dean-Stark apparatus. The reaction mixture was poured into 5% Na_2CO_3 (100 ml) and washed thoroughly. The organic layer was dried over K_2CO_3 and removed in vacuo to give a white solid. Yield 92%, mp 72–73 °C. MS-APCI: $[M+H]^+$ 243.3 (242.0). ^1H NMR ($CDCl_3$): 7.51–7.48 (2H, d, $J = 8.3$ Hz), 7.37–7.34 (2H, d, $J = 8.3$ Hz), 5.46 (1H, s), 4.25–4.23 (2H, m), 4.02–3.93 (2H, m), 2.22–2.15 (1H, m), 1.58–1.42 (1H, m). ^{13}C NMR ($CDCl_3$): 122.7, 117.5, 114.7, 110.6, 92.8, 65.7, 32.0.

5.1.3.2. 4′-(4-Methylpiperazin-1-yl)benzaldehyde.[6] A Schlenk flask was charged with 2-(4-bromophenyl)-1,3-dioxane (1.0 mmol), 1-methylpiperazine (1.1–1.2 mmol), sodium *tert*-butoxide (1.4 mmol), tris(dibenzylidene acetone)dipalladium (0) (0.0025 mmol, 0.5% Pd), rac-BINAP (rac-2,2′-bis(diphenylphosphino)-1,1′-binaphthyl) (0.0075 mmol), and toluene (2 ml) under argon. The flask was immersed in an oil bath (80 °C) and stirred until the starting materials had been completely consumed as judged by TLC (10 h). The solution was then allowed to cool to room temperature, extracted with CH_2Cl_2, and the crude product purified by flash chromatography on silica gel. Yield: 81 %. Mp 58–60 °C. MS-APCI: $[M+H]^+$ 205.4 (204.1). ^1H NMR ($CDCl_3$): 9.79 (1H, s, CHO), 7.77–7.74 (2H, d, $J = 8.6$ Hz), 6.94–6.91 (2H, d, $J = 8.6$ Hz), 3.44–3.40 (2H, t), 2.57–2.54 (2H, t), 1.65 (3H, s). ^{13}C NMR ($CDCl_3$): 190.4, 155.0, 131.8, 127.1, 113.5, 54.6, 47.0, 46.1.

5.2. Molecular modeling and collation of physicochemical parameters

The pK_a values of the various ionizable groups in the chalcone library were estimated with ACD/pKaDB found in ACD/I-Lab Version 6.0 for Microsoft Windows. With this information, the chalcones were constructed in their predominant ionized states at pH 7.0 using the fragments found in the Sybyl 7.0 (Tripos Inc., St. Louis, MO). They were geometry optimized using the standard Tripos force field with a distance dependent dielectric function until a root mean square deviation of 0.001 kcal/ mol Å was achieved.

Area, polar volume, C$\log P$, molar refractivity, partial positive and partial negative surface areas were computed for these compounds. The compounds were again drawn and minimized using the Molecular Modeling Pro Plus Version 6.2.3 (ChemSW, Fairfield, CA) forcefield (MM2) for the determination of width, length, breadth, area, polar surface area, molecular volume, dipole moment, hydrogen bonding parameters (H bond donor, H bond acceptor, Hansen H bonding), % hydrophilic surface, CNDO $\log P$, Crippen $\log P$, $\log P$, HOMO, LUMO, connectivity indices (0, 1, 2, 3, 4), kappa 2 shape index. The charge on the α and β carbons was determined from Chem 3D Ultra 10.0 from chalcones drawn and minimized in their uncharged states. The projection methods (PCA and PLS) were carried out on SIMCA-P 11 (Umetrics AB, Umea, Sweden) with default settings. MLR and correlation analyses were run on SPSS 15.0 (SPSS Inc., Chicago, IL).

5.3. Microculture tetrazolium assay for determination of antiproliferative activity

Growth inhibitory activities were determined on the following cell lines: HCT 116 (transformed human colon cancer cells, gift from Dr. Balram Chowbay, National Cancer Centre, Singapore), MCF 7 (human breast cancer cells, American Type Culture Collection, Rockville, MD, USA) and CCL 186 (normal human diploid embryonic lung fibroblasts, American Type Culture Collection, Rockville, MD, USA). Microculture tetrazolium assay was based on the ability of metabolically viable cells to reduce the yellow tetrazolium salt (MTT) to colored formazan crystals.[12] The procedure was carried out as described earlier.[4] Each compound was tested at no less than eight concentrations, with at least three runs for each concentration. IC_{50} values were determined using Prism GraphPad (San Diego, CA, USA).

5.4. Cell cycle analysis

Chalcones **1-123**, **6-130**, and **7-140** at 0.5 and 5 μM were tested for their effects on the cell cycle of HCT 116. The procedure described in Ref. 4 was followed.

5.5. Statistical analysis

Independent sample *t*-test run (SPSS 15.0, SPSS Inc., Chicago IL) was used to test for significant differences in IC_{50} values.

Acknowledgments

Liu XL gratefully acknowledges National University of Singapore (NUS) for granting her a research scholarship for graduate studies. This work was supported by Grant RP 148 000042112 from NUS.

Supplementary data

Supplementary data associated with this article can be found, in the online version, at doi:10.1016/j.bmc.2007.07.042.

References and notes

1. Xia, Y.; Yang, Z. Y.; Xia, P.; Bastow, K. F.; Nakanishi, Y.; Lee, K. H. *Bioorg. Med. Chem. Lett.* **2000**, *10*, 699.
2. Pati, H. N.; Holt, H. L.; LeBlanc, R.; Dickson, J.; Stewart, M.; Brown, T.; Lee, M. *Med. Chem. Res.* **2005**, *14*, 19.
3. Dimmock, J. R.; Jha, A.; Zello, G. A.; Allen, T. M.; Santos, C. L.; Balzarini, J.; De Clercq, E.; Manavathu, E. K.; Stables, J. P. *Pharmazie* **2003**, *58*, 227.
4. Liu, X. L.; Go, M. L. *Bioorg. Med. Chem.* **2006**, *14*, 153.
5. Craig, P. N. *J. Med. Chem.* **1971**, *15*, 680.
6. Nielsen, S. F.; Larsen, M.; Boesen, T.; Schonning, K.; Kromann, H. *J. Med. Chem.* **2005**, *48*, 2667.
7. Wolfe, J. P.; Buchwald, S. L. *J. Org. Chem.* **2000**, *65*, 1144.
8. Kamila, S.; Mukherjee, C.; Mondal, S. S.; De, A. *Tetrahedron* **2003**, *59*, 1339.
9. Pharmacokinetics In Silico (phakiso) software, http://www.phakiso.com/.
10. Livingstone, D. In *Data Analysis for Chemists*; Oxford University Press: New York, 1995, Chapters 4 and 8.
11. Lawrence, N. J.; McGown, A. T.; Ducki, S.; Hadfield, J. A. *Anti-Cancer Drug Des.* **2000**, *15*, 135.
12. Alley, M. C.; Scudiero, D. A.; Monks, A.; Hursey, M. L.; Czerwinski, M. J.; Fine, D. L.; Abbott, B. J.; Mayo, J. G.; Shoemaker, R. H.; Boyd, M. R. *Cancer Res.* **1988**, *48*, 589.